Union College
Union | Digital Works

Honors Theses | Student Work

6-2007

Synthesis and structural characterization of isotopically labeled asymmetric metal complexes : through metal coupling of NMR active nuclei

Jenna Lynn Welby
Union College - Schenectady, NY

Follow this and additional works at: https://digitalworks.union.edu/theses

 Part of the Chemistry Commons

Recommended Citation
Welby, Jenna Lynn, "Synthesis and structural characterization of isotopically labeled asymmetric metal complexes : through metal coupling of NMR active nuclei" (2007). *Honors Theses*. 2101.
https://digitalworks.union.edu/theses/2101

This Open Access is brought to you for free and open access by the Student Work at Union | Digital Works. It has been accepted for inclusion in Honors Theses by an authorized administrator of Union | Digital Works. For more information, please contact digitalworks@union.edu.

(QA
82
W435
2007

SYNTHESIS AND STRUCTURAL CHARACTERIZATION OF ISOTOPICALLY LABELED ASYMMETRIC METAL COMPLEXES: THROUGH METAL COUPLING OF NMR ACTIVE NUCLEI

By

Jenna Lynn Welby

Submitted in partial fulfillment
of the requirements for
Honors in the Department of Chemistry

UNION COLLEGE
June 2007

ABSTRACT

WELBY, JENNA. Synthesis and Structural Characterization of Isotopically Labeled Asymmetric Metal Complexes: Through Metal Coupling of NMR Active Nuclei

Structure elucidation of a substance can be vital toward understanding chemical properties and reactivity. Nuclear Magnetic Resonance (NMR) Spectroscopy has played a significant role in the structural determination of organic, inorganic, and biological compounds. A search of the literature revealed that only minimal information is available regarding the use of isotopically-labeled nuclei to aid in structure determination of inorganic complexes. The basic information that is lacking includes relevant chemical shifts and scalar coupling constants. Our studies have begun to compile such information utilizing two different methods: first, synthesizing asymmetric tetradentate ligand frames and second, utilizing sterically bulky ligand frames. Each method introduces asymmetry to the corresponding complex and positions isotopically labeled ligands trans to each other. ^{13}C NMR studies on a dicyano ($^{13}CN^-$) complex that we have characterized reveal that isotopically labeled ligands positioned trans to each other can couple through the metal center with a $^2J_{C-C}$ value of 44 Hz. This value agrees very well with the theoretical value of 46 Hz. A search of the literature indicates that this is the largest two bond carbon-carbon scalar coupling reported to date and only the second example of a metal complex to exhibit through metal coupling of isotopically labeled ligands. We have also synthesized and characterized two more asymmetric complexes which have been structurally characterized. The results of these studies will be presented and along with overall implications of the use of isotopically labeled ligands to aid in structure determinations.

INTRODUCTION

Structure determination is an ongoing task in the field of chemistry as knowledge of chemical structure provides unprecedented information towards understanding a substance's chemical properties and reactivity. Thus, the tools and techniques that aid in structure determination are vital to an array of chemical studies. The analysis of the interactions between energy and molecules through spectroscopy can provide detailed information about molecular structure. Nuclear magnetic resonance (NMR) spectroscopy has evolved into a primary source of identification in organic, inorganic, and biological settings.[1-7]

NUCLEAR MAGNETIC RESONANCE SPECTROSCOPY

NMR spectroscopy was first introduced commercially in 1952. At that point the NMR instrument had a very narrow range of capabilities and applications. It consisted of a small magnet that was used for studying the protons of highly concentrated organic compounds.[8] The function of NMR spectroscopy was limited to compound identification, structural characterization, and testing for impurities in synthetic preparations.

The proton remains the most common nucleus studied with NMR spectroscopy, yet applications of the technique have evolved, and as such, nuclei including ^{10}B, ^{11}B, ^{13}C, ^{14}N, ^{15}N, ^{19}F, and ^{31}P, are routinely measured.[9-10]

The instrumental abilities advanced with the introduction of larger magnets capable of detecting the structures of 3-D proteins as large as 900,000 Da. NMR has

been used in a broad array of studies, ranging from interpreting macromolecules and the active-site chemistry of proteins to studying the nutritional values of dog food.[11-12]

Nuclear magnetic resonance is also a critical investigative technique in the design of pharmaceuticals, metabolite identification, and drug-receptor interactions. The review by Pochapsky and Pochapsky includes a detailed overview of the methods of NMR that are currently at the forefront of the pharmaceutical industry.[13] NMR spectroscopy is now used to detect macromolecular structure and dynamics as well as the interactions between small molecules and receptors. These features are key to studies of biological advancement.

NMR instruments have become still more advanced through the introduction of tandem NMR techniques. NMR instruments have been coupled to such detectors as gas chromatographs and mass spectrometers, thus increasing the separation and characterization efficiencies of the instruments.[8] With such great advances, NMR spectroscopy has become a primary source of data in many branches of science.

Nuclear magnetic resonance spectroscopy is founded on the principle that when a sample is placed in a magnetic field, the nuclei of certain atoms absorb the radiowaves emitted by the field. The absorbed energy is not sufficient to vibrate, rotate, or electronically excite the molecules or atoms, yet it is enough to influence the atoms' nuclear spin. Such absorption and associated spin alteration is termed magnetic resonance.

The ability of the NMR spectrometer to probe a nucleus depends on the nucleus' spin characteristics, specifically the spin quantum number. When a nucleus has an even atomic weight and an even charge, the spin quantum number is zero. Such a nucleus has

no spin, nor angular momentum, and thus, this spin state can not be altered and radiowaves are not absorbed. Alternately, when the atomic weight is even and the charge is odd, the spin quantum number will be an integer. In this case the nucleus will not impart spin on the molecule. The third possibility for the spin quantum number is when both the atomic weight and charge of a nucleus are odd. This will cause the spin quantum number to be an integer multiple of ½. When the spin quantum number is fractional, the nucleus will absorb radiowaves and the nucleus is termed NMR active.

When NMR active nuclei are placed in a strong, uniform magnetic field, they align in a well defined pattern that corresponds to a quantized energy level. In the energy level, the nuclei have spin states that are parallel to the magnetic field. Upon absorption of electromagnetic energy, such nuclei are excited, causing a spin flip and alignment anti-parallel to the magnetic field. The nuclei eventually release the absorbed energy and return to their initial spin states. The rate at which a given nucleus returns to its initial spin state is mathematically interpreted using Fourier transformations.[8] Fourier transformations are used to convert information from the time domain to the frequency domain. When nuclear information gathered using the NMR spectrometer is presented in the frequency domain, a spectrum that is characteristic of a given sample is produced. The main spectral characteristics are chemical shift, peak integration, and coupling. Through interpreting the collection of these characteristics, the importance of an NMR spectrum in structure determination becomes evident.

Chemical shift refers to the peak position in an NMR spectrum. Peaks in NMR spectra are found over a range of chemical shifts because nuclei in different molecular environments absorb characteristic frequencies of energy. The electronic environment of

an NMR active nucleus refers to the electron density surrounding the nucleus. The electrons around a nucleus create a magnetic field which opposes the field given off by the instrument and the nucleus is said to be shielded. Based on variations in bond characteristics and the identities of adjacent atoms, NMR active nuclei are shielded to different degrees and peaks are positioned at characteristic locations in the spectrum.

When an NMR active nucleus is in close proximity to an electronegative atom, the inductive effects of the electronegative atom pull electron density away from the nucleus. As such, the nucleus is deshielded and experiences a greater magnetic influence. The signal produced from a shielded nucleus will be positioned upfield in an NMR spectrum, while the signal for a deshielded nucleus will be positioned downfield in an NMR spectrum.

Peak integration is a key feature of NMR spectra. The relative integral areas beneath different peaks in NMR spectra can be compared. The ratio of the areas of two separate peaks indicates the number of nuclei causing one signal relative to the number of nuclei causing the second signal.

A third major characteristic of NMR spectra is signal splitting. This phenomenon arises from the indirect coupling of neighboring NMR active nuclei. Splitting, or coupling, of an NMR active nucleus is caused by other nuclei that are in different environments while being fewer than three bond lengths away. It entails the splitting of signals as a result of adjacent nuclei possessing multiple spin orientations. Signal splitting generally has no impact on ^{13}C NMR spectra as it is rare that NMR active carbon nuclei are found in close proximity within a molecule given that the relative abundance of ^{13}C in nature is approximately 1.1%. A key feature associated with signal splitting is the

magnitude of the separation between peaks, the J-constant, which offers insight into the magnetic interaction between the coupled nuclei.

The J-constant, which is referred to as the coupling constant, or the spin-spin coupling constant, can be measured directly from an NMR spectrum. The J-value is an indicator of which protons are causing the splitting in NMR spectra. The magnitude of the J-coupling constant is independent of magnetic field strength and thus can be useful regardless of the strength of an NMR instrument. For protons bound to adjacent, singly bound carbons, J typically has a value between 6 and 8 Hz. The introduction of double bonds and aromatic rings cause adjacent protons to have larger coupling constants and to experience longer range coupling.[8]

Carbon-13 nuclei are expected to split one another as they possess two spin states. However, this phenomenon is rarely seen due to the low natural abundance of carbon-13. Using isoptocially enriched molecules or special techniques, $^{1}J_{C\text{-}C}$ values ranging from 20 to 200Hz have been measured.[8]

BIOLOGICAL IMPLICATIONS OF NMR

In addition to an expansion in the instrumental uses of NMR spectroscopy, the applications of NMR spectroscopy have become more widespread in recent years. Many biological systems of interest contain active site metals (paramagnetic and diamagnetic alike) and NMR has been used as an investigative technique to probe the metal coordination sphere, electronic structure and reaction mechanisms. An article published by Moon and Richards is an early example of such a biologically imperative application.[14] The effect of binding ^{13}C-enriched carbon monoxide to various

hemoglobins was studied with NMR spectroscopy. The researchers presented spectroscopic evidence that carbon monoxide interacts differently with various hemoglobin subunits. The NMR spectra in Figure 1 show that based on the identity of the hemoglobin subunit there is great variation in the shape and position of the carbon monoxide peak.

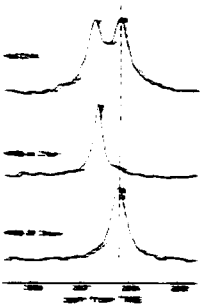

Figure 1. Spectra of the ^{13}CO resonances of a sample of intact human adult hemoglobin and the isolated HbB chromines of its alpha and beta subunits.

A more recent study using NMR spectroscopy was presented in the work by H. Fuji.[15] In this work, ^{13}C NMR spectroscopy was used to study the nature of the proximal ligand in ferric heme proteins. The study focused on a series of heme proteins containing isotopically labeled $^{13}CN^-$ in the proximal position which differed only in the identity of the atoms hydrogen bonded to a histidine residue. These complexes were compared using NMR spectroscopy. Isotopically enriched $^{13}CN^-$ proved a sensitive probe for studying ferric heme proteins. The researchers provided evidence that there was a large chemical shift in the ^{13}C resonance of $^{13}CN^-$ despite very slight variations in the imidazole groups ligated trans to the cyanide. This study showed the great sensitivity of the NMR spectrometer.

OTHER PHYSICAL METHODS

When the information provided by NMR spectroscopy is insufficient for structural determination, other instrumental techniques may be introduced. X-ray structural analysis, infrared absorption spectroscopy (IR) and ultraviolet/visible absorption spectroscopy (UV/VIS) are useful physical characterization methods.

X-ray structural analysis is a phenomenal technique because it allows for the structural elucidation of small molecules without ambiguity. Unlike NMR spectroscopy, X-ray analysis requires the presence of suitable crystals for diffraction.

Most organic and inorganic compounds, minerals, metals, and alloys, and many types of polymers can be found in crystalline form and thus be analyzed with X-ray diffraction.[16] Crystallization of biological entities and synthetic inorganic complexes is a trial-and-error process that is made difficult by impurities and a lack of knowledge as to the process of crystal formation. For a crystal to be suitable for x-ray diffraction analysis, it must have a well-defined lattice of ions or molecules.

Once a suitable crystal is obtained, it is placed in a monochromatic X-ray beam. The X-ray waves diffract away from the crystal according to the positions of the atoms within the lattice. The diffraction pattern is then interpreted and the structure of the molecule is found. The development of this analytical technique, termed X-ray crystallography, has been invaluable in structure determination.

IR spectroscopy is a characterization technique that uses energy from the infrared region of the electromagnetic spectrum to vibrate chemical bonds. The frequency at which a chemical bond vibrates is determined by the identities of the bonds' atoms as well as the bond order. The characteristic vibrational frequencies of various chemical entities can be used to determine the presence or absence of specific atoms. Slight variations in vibrational frequencies can indicate whether or not a small ligand is bound to a larger complex.

The application of IR spectroscopy to bonding characteristics is presented nicely in the work by Penner-Hahn et. al. who studied cyanocuprates with IR spectroscopy.[17] It

was explained that the formation of strong sigma bonds resulted in increased IR absorption frequency as a result of a withdrawl of pi* electron density. Alternately, lowering the electronegativity or oxidation state of a metal leads to a decrease in IR absorption frequency due to increased pi* back bonding to the metal center. This decrease is typically on the order of 20-40 cm^{-1}. The following IR stretching frequencies were reported for cyanide complexes: solid KCN, 2049cm^{-1}, aqueous CN^-, 2080 cm^{-1}, solid CuCN, 2172cm^{-1}, aqueous $Cu(CN)_2^{-1}$, 2124 cm^{-1}. This suggests that upon binding to a metal center, the infrared stretching frequency of CN^- shifts to a higher value. Thus, an IR spectrum can provide insight into the binding situation in a chemical setting.

UV/VIS absorption spectroscopy provides useful information regarding the electronic structure of molecules. Using this technique, samples are irradiated with photons whose energies fall in the visible and near ultraviolet regions of the electromagnetic spectrum. Some of the incident light is absorbed by the sample, while other light passes through unimpeded. The instrument determines the ratio of the intensity of light passing through a sample to the intensity of light emitted by the instrument. This ratio is called the transmittance. The instrument produces a spectrum relating absorption, a quantity directly dependent on transmittance, to wavelength. The absorption pattern of this spectrum can explain electron transitions and the presence or absence of extended conjugation of a molecule. The locations of absorbance maxima are dictated by the identity of species within the molecule.

The Beer-Lambert law is an empirical relationship between the absorption of light at a particular wavelength and the characteristics of the material through which the light is passing. This law is expressed with an equation in which A is the absorbance, ε is the

molar absorptivity with units of $M^{-1}cm^{-1}$, *l* is the path length through solution with units of cm, and c is the concentration of the absorbing species, with units of M.

$$A = \varepsilon * l * c$$

Molar absorptivity measures how strongly a chemical species absorbs light at a particular wavelength. This property is intrinsic of the species and can be measured and reported at a series of maximal wavelengths.

The aforementioned instrumental techniques are extremely important in the chemistry of structure determination. With instrumental analysis, chemical entities whose structures could not be determined in the past can now be discerned with relative certainty.

INORGANIC MODEL COMPLEXES

Inorganic model complexes are synthesized to provide information regarding the structure and/or electronic state of biomimetic metal complexes which can be correlated to data acquired for the original biological entity. These studies are advantageous because they allow for the interpretation of small molecules rather than bulky metalloenzymes and proteins which are difficult to isolate and purify. Such syntheses also allow for studies of intermediates which can not be isolated in vivo.[15] Using such models, biological systems can be better understood. A report of such model complexes was presented by Walker and co-workers. This study defined the electronic ground state of ferric porphyrin complexes (which parallel heme containing proteins) using NMR, electron paramagnetic resonance (EPR), Mössbauer and magnetic circular dichroism techniques (MCD).[18-20] This work was extended later by Nakamura and co-workers who

reported that ^{13}C chemical shifts of coordinated cyanide ligand to ferric porphyrin could be used in determining the electron configuration around a metal center.[21]

Another example of an inorganic model complex can be seen in a study conducted by Ye et al.[22] This research group utilized ^{13}C NMR spectroscopy to identify carboxylate binding modes in zinc model complexes of carbonic anhydrase and carboxypeptidase A. The report showed chemical shifts of 184, 180 and 176 ppm for chelating, bidentate and monodentate bridging modes. It was shown that a ^{13}C NMR spectrum could be used to ascertain binding modes through the dependence of the chemical shift on bond order and electron density. This information goes beyond the scope of the sample studied and can be used to model the binding modes of other samples.

METAL CYANIDE COMPLEXES

Cyanide-containing transition metal complexes have recently become of great interest in a diverse array of chemical areas, namely molecular magnetism and the synthesis of porous supramolecular assemblies.[22] Although cyanide has a high toxicity rating and is extremely dangerous to the central nervous system, it is widely used in industry. Uses of cyanide include mining, metallurgy and photographic processing, as well as the production of nitriles, nylon and acrylic plastics.[9]

In addition to its uses in industrial processes, cyanide species are important in organic syntheses, enzyme active sites, high-temperature superconductors, and zeolite-like inorganic structures that undertake house-guest chemistry.[23] The vitality of cyanide stems from the fact that it is one of the strongest ligands in the spectrochemical series.

Cyanide reacts with virtually any metal complex by replacing the ligands already bound to a metal center. Therefore it is of interest to develop a greater understanding of the chemistry of the cyanide ligand.

Steps towards understanding the chemistry of cyanide are being undertaken using multinuclear NMR. In work by Bryce et al. ^{13}C and ^{15}N solid-state NMR spectroscopies were used to investigate the structure of silver cyanide.[1] Results generated indicate that there is indirect spin-spin coupling between different nuclei within the molecule when isotopically labeled ligands are utilized. The investigation also studied the connectivity of the ligand to the metal center by combining the results from different NMR spectral analyses.

CURRENT RESEARCH

Bearing in mind the substantial growth in the capabilities of structural elucidation arising from advances in NMR spectroscopy, as well as advantages of studying inorganic model complexes, a synthetic inorganic research project was devised. A search of the literature indicated that minimal information was available regarding the use of isotopically-labeled ligands to aid in structure determination. Particularly, little has been reported involving the use of multiple isotopically labeled ligands, and no scalar coupling information is available in this area. Without access to such values arises their inability to aid in structure determination in inorganic as well as bioinorganic chemistry.

This research project involves compiling such information which aims at providing valuable insight into chemical structure. This information could have a profound impact on the ability to determine ligand substitution in metal-containing species as well as providing definitive information regarding the geometric arrangement of ligands around a metal center. Once established the peak positions and magnitude of scalar coupling constants in ^{13}C NMR spectra can be used in structure determination in inorganic model complexes, with subsequent application to biological systems.

In our efforts to study the effects of isotopically labeled ligands on scalar coupling in NMR spectra, we designed set of asymmetric metal complexes. The metal center used in this study was cobalt in the (III) oxidation state. Cobalt (III) is an ideal metal center because it contains six d-electrons in a low spin configuration. As such, it is diamagnetic and thus easily studied with NMR spectroscopy. With such an electron configuration, cobalt (III) is particularly prone to an octahedral geometry, the geometry that is required in our study of asymmetric metal complexes.

It was necessary that our complexes be asymmetric as scalar coupling only takes place when the nuclei involved in coupling are present in different electronic environments. Through imparting a degree of asymmetry, NMR active nuclei positioned trans to each other in octahedral geometries are able to couple one another.

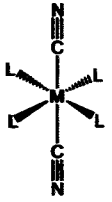

Trans

Figure 2. General representation trans- configuration in octahedral metal complexes where M represents the metal center and L represents the ligand frame.

The syntheses of asymmetric metal complexes that impart trans configurations of isotopically labeled ligands were designed with two methods. The first method involved the synthesis of tetradentate ligand frames which afforded asymmetry on the basis of the stereochemistry of the backbone. The second method utilized sterically bulky ligand frames that generated asymmetry through preventing ligand frame rotation.

The results of these studies are presented.

EXPERIMENTAL

Physical Measurements.

Infrared Spectra were obtained with an Avatar 330 FTIR spectrophotometer. Absorption spectra were measured on a HP Diode Array spectrophotometer. ^{1}H NMR and ^{13}C NMR spectra were recorded on a Gemini 200 mHz FT NMR spectrometer.

Preparation of Compounds.

All solvents were purchased dried. The ligand $PyPSH_4$ and metal complex $(Et_4N)_2[Co_2(PyPS)_2]$ were synthesized following published procedures.[24,25] NEt_4CN was purchased from Aldrich Chemical Company.

$Et_4NS^{13}CN$.

A batch of 1.04 g (1.07 mmol) $KS^{13}CN$ was added to a 100 mL round bottom flask with 20 mL anhydrous methanol. NEt_4Cl was dissolved in 20 mL anhydrous methanol. Then the NEt_4Cl solution was added dropwise to $KS^{13}CN$ mixture and the reaction was stirred for 20 min. White KCl solid was removed using a fine frit. The methanol solvent was removed via rotary evaporation under a vacuum and the product was isolated in quantitative yield. An analogous reaction was carried out with non-isotopically labeled starting material. ^{1}H NMR spectrum ($CDCl_3$, 200 MHz) δ from TMS: 1.4 (m), 3.5 (m). ^{13}C Spectrum (DMSO, 50.28 MHz) δ from TMS: 131.28. Selected IR band: isotopically labeled product (ν, cm^{-1}): 2126 ($\nu_{C\equiv N}$). Selected IR band: non-isotopically labeled product (ν, cm^{-1}): 2056 ($\nu_{C\equiv N}$).

Meso-1,2-diphenylethylenediiminomethylphenol (MDEDS) (1).

A batch of 0.996 g (4.691 mmol) of the ivory powder (98%) meso-1,2-diphenylethylenediamine was dissolved in 15 mL anhydrous ethanol in a 100 mL round bottom flask. Next, 1.50 mL (14.31 mmol) of salicylaldehyde was added dropwise to the reaction vessel using a digital pipette in two aliquots of 0.750 mL. A yellow precipitate formed immediately following the addition. The reaction was capped and stirred for 17 h. The microcrystalline solid was collected via gravity filtration and washed first with ethanol then with 5 mL ether. The bright yellow crystals were dried under vacuum for 1 h. Yield: 92.5% (1.825 g). ^{1}H NMR spectrum ($CDCl_3$, 200 MHz) δ from TMS: 4.75 (s), 6.80 (t), 6.92 (d), 7.08 (d), 7.27 (m), 8.09 (s), 13.12 (s). Selected IR bands (v, cm^{-1}): 1620 ($\nu_{C=N}$).

[Co(MDEDS)] (2).

A batch of 0.194 g (0.499mmol) of **1** was measured into a Schlenk flask with stir bar. The flask was degassed and 15 mL anhydrous methanol added. The heterogeneous solution in the flask was further degassed by switching from nitrogen to vacuum three times. After 20 min, 0.124 g (0.449 mmol) of cobalt (II) acetate tetrahydrate was added to the mixture, which immediately turned brown. Next, 10 mL anhydrous methanol was added and the solution turned dark red/orange as a precipitate formed. The red/orange mixture was stirred for 18 h and then the crystals were collected on a Schlenk frit and dried under high vacuum. Crystals suitable for x-ray analysis were obtained by dissolving **2** in methylene chloride with slow diffusion of diethyl ether. Selected IR bands (v, cm^{-1}): 1622 ($\nu_{C=N}$). Electronic absorption spectrum: λ_{max} (nm) (ε, $M^{-1}cm^{-1}$)

(methylene bromide): 418 (15432), 356 (13867), 356 (13261); (methylene chloride): 373 (12872), 291 (24677), 272 (22452).

[Co(MBEDS)(CN)$_2$] (3).

A batch of 0.050 mg (0.105 mmol) of **2** was weighed into a 25 mL roundbottom flask with stirbar to which 15 mL anhydrous acetonitrile were added. In a separate vial, 0.039 mg (0.251 mmol) of ^{13}C enriched tetraethylammonium cyanide ($NEt_4{}^{13}CN$) was dissolved in anhydrous acetonitrile. The $NEt_4{}^{13}CN$ solution was pipetted dropwise into the roundbottom. Upon addition of the $NEt_4{}^{13}CN$, the solution turned from brown to orange. The mixture was refluxed for 1.5 h during which it changed color to dark red. The solvent was removed under vacuum and the product left to dry overnight. ^1H NMR spectrum (DMSO, 200 MHz) δ from TMS: 1.14 (m), 1.76 (s), 3.19 (m), 5.45 (s), 6.26 (t), 6.73 (d), 6.92 (sc), 7.13 (m), 7.32 (m). Selected IR bands (ν, cm^{-1}): 2122 ($\nu_{C\equiv N}$).

[(Et$_4$N)$_2$[Co(PyPS(SO$_2$))]$_2$ (4).

A portion of 0.300 g (0.261 mol) $(Et_4N)_2[Co_2(PyPS)_2]$ was weighed out into a 50 mL round bottom flask and dissolved in 20 mL anhydrous methanol. Next, 750 μL 30% H_2O_2 were added and the reaction vessel was immediately capped. After 2 h the volume of the solution was reduced to approximately 10 mL. Crystals suitable for x-ray analysis were obtained by slow diffusion of diethyl ether into methanol. After 24 h, long, thin black crystals were collected. ^1H NMR spectrum (DMSO, 200MHz) δ from TMS: 1.14 (m), 3.17 (m), 3.38 (s), 5.14 (d), 6.31 (t), 6.85 (t), 6.99 (t), 7.07 (t), 7.38 (s), 7.75 (d), 7.79 (d), 8.15 (t), 8.42(d). ^{13}C NMR spectrum (DMSO, 50.28MHz) δ from TMS: 119.62, 121.13, 121.31, 122.31, 123.43, 125.13, 125.80, 128.59, 130.07, 131.90, 137.80, 174.75,

150.80, 154.43, 154.56, 158.11, 164.59, 170.05, 191.25. Selected IR bands (ν, cm^{-1}): 1601, 1586 ($\nu_{C=O}$), 1453, 1357 ($\nu_{S=O}$).

$(Et_4N)_3[Co(PyPS(SO_2))(CN)_2]$ (5).

A portion of 97 mg (0.08 mmol) of 4 was dissolved in 10 mL anhydrous acetonitrile in a 50 mL round bottom flask. Then a batch of 75 mg (0.48 mmol) of Et_4NCN, dissolved in 3 mL anhydrous acetonitrile, was added to it. The reaction was refluxed. After 2 h, the heat was removed and the solution stirred for an additional 3 h. The solvent was then removed using rotary evaporation and dried under high vacuum for 18 h. Note: isotopically enriched $NEt_4{}^{13}CN$ was used to make the isotopically labeled derivative, 6. ^1H NMR spectrum (DMSO, 200MHz) δ from TMS: 2.07 (s), 3.18 (m), 6.52 (t), 6.77 (d), 7.05 (m), 7.35 (d), 7.56 (d), 7.81 (m), 8.15 (t), 8.71 (d). ^{13}C NMR spectrum (isotopically labeled product, DMSO, 50.28MHz) δ from TMS: 139.8, 141.7. Selected IR bands (ν, cm^{-1}): 2120 ($\nu_{C\equiv N}$), 1578 ($\nu_{C=O}$), 1452, 1360 ($\nu_{S=O}$).

Results and Discussion

♣ MDEDS Ligand Synthesis

The synthesis of the meso-1,2-diphenylethylenediiminomethylphenol (MDEDS) ligand was carried out through combining meso-1,2-diphenylethylenediamine and salicylaldehyde under anhydrous conditions (Scheme 1).

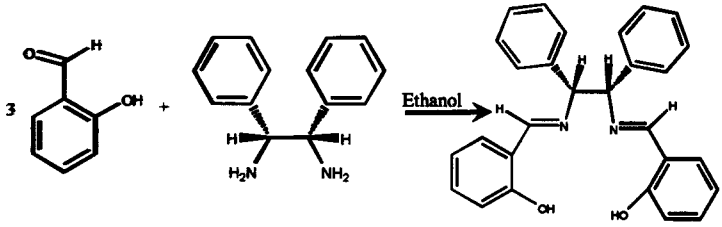

Salicylaldehyde | Meso-1,2-diphenyl ethylenediamine | MDEDS

Scheme 1. Synthesis of MDEDS ligand.

Three equivalents of salicylaldehyde were added to insure that there was no unreacted meso-1,2-diphenyl ethylenediamine starting material in the reaction vessel. This reaction proceeded instantly as evidenced qualitatively by the immediate color change to yellow and precipitate formation following the addition of salicylaldehyde to meso-1,2-diphenyl ethylenediamine. The reaction stirred for 17 h to insure that it went to completion. It was then filtered and rinsed with ethanol to remove any unreacted salicylaldehyde starting material. A subsequent rinse with ether was done for the sake of drying. After the solvent was removed via gra· ity filtration, spectroscopic analyses were carried out. A ^{1}H NMR spectrum of MDEDS is shown (Figure 3).

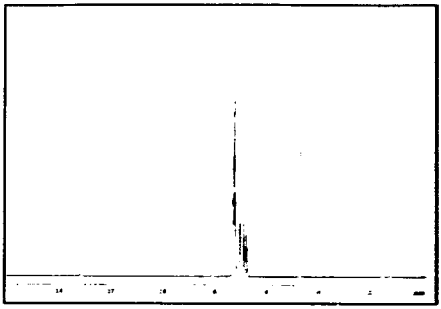

Figure 3. ^{1}H NMR spectrum of MDEDS in $CDCl_3$ on a 200 MHz instrument.

In the ^{1}H NMR spectrum the two doublets and a triplet around 7 ppm are generated by the phenyl protons that are present on the ligand backbone. The multiplet at 7.3 ppm is caused by the phenol protons. The singlet at 8.1 ppm is assigned to the imine hydrogen. This signal was not present in either of the starting materials, thus providing further evidence that the reaction took place. Finally, the peak at 13.12 ppm is assigned to the alcohol protons. This assignment was confirmed through carrying out a D_2O wash. A ^{1}H NMR spectrum of MDEDS following the D_2O wash is shown in Figure 4.

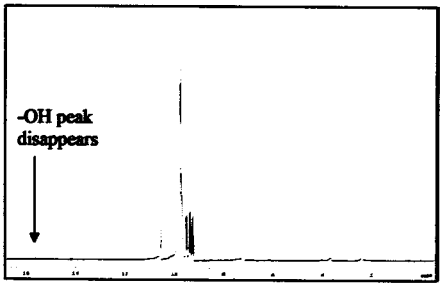

Figure 4. ^{1}H NMR of MDEDS in $CDCl_3$ on a 200MHz instrument following D_2O wash.

During the deuterium oxide wash the proton atom of the alcohol is replaced with a deuterium atom. The NMR spectrum of the D_2O washed ligand does not have the –OH peak.

An infrared spectrum of the MDEDS ligand was also collected (Figure 5).

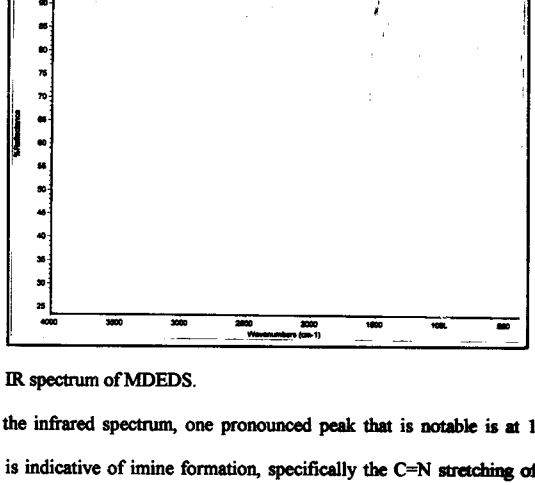

Figure 5. IR spectrum of MDEDS.

In the infrared spectrum, one pronounced peak that is notable is at 1620 cm^{-1}. This peak is indicative of imine formation, specifically the C=N stretching of an imine bond. Additionally, the broad peak centered at 2850 cm^{-1} is assigned to the O-H stretching of the phenol alcohol.

The MDEDS ligand contains a large empty space in the center of the frame into which a metal can enter and assume a square planar geometry. This reaction would occur readily following the deprotonation of the OH group. Once complexed, the MDEDS ligand frame imparts asymmetry due to the presence of the two phenyl rings. In one plane, the large, bulky phenyl groups are present, while in the other, small protons take

up minimal space. Thus, the ligand frame affords asymmetry by virtue of the stereochemistry of the backbone. Equipped with asymmetry, this ligand frame can be used to generate the different electronic environments required to observe the coupling between two nuclei positioned in the apical sites in the metal complex.

Co(MDEDS) Synthesis

The metallation of the MDEDS involved a reaction between MDEDS and Co(II) acetate tetrahydrate. This reaction was carried out under anaerobic conditions because of the propensity of Co(II) to air oxidize. The synthetic pathway involved in this reaction can be seen in Scheme 2.

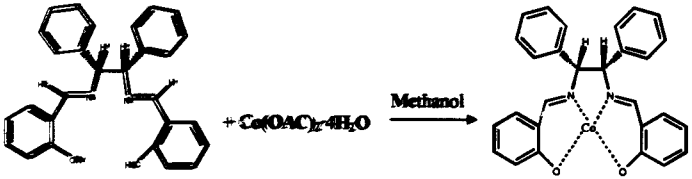

Scheme 2. Synthesis of Co(MDEDS).

The reaction took place immediately as evidenced by the color change from yellow to orange. NMR analysis was not possible for this compound as it contains a paramagnetic Co (II) metal center. The infrared spectrum was collected (Figure 6).

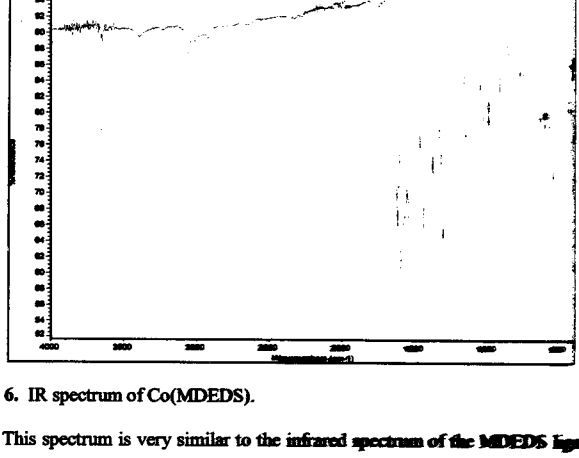

Figure 6. IR spectrum of Co(MDEDS).

This spectrum is very similar to the infrared spectrum of the MDEDS ligand, the most visible difference being that it lacks the broad –OH stretching frequency at 2850 cm^{-1}. This is suggestive of complex formation, as the alcohol group is deprotonated during the reaction. Also, there was a shift in the $\nu_{C=N}$ stretching frequency from 1620 cm^{-1} to 1622 cm^{-1}. This shift to higher energy is caused by the metal, which increases the mass bound to the imine nitrogen. Because the imine nitrogen feels a higher relative mass, more energy is required to stretch the imine bond.

Recrystallization of Co(MDEDS) was carried out in methylene chloride with slow diffusion of diethyl ether. After 2 days, red crystalline blocks were obtained. The Co(MDEDS) crystal structure is shown (Figure 7). The asymmetry that is imparted by the ligand frame backbone can be clearly seen as the two phenyl rings stretch out of the plane of the paper, while the two proton atoms go into the plane. Select bond distances and angles for this complex are shown (Tables 1 and 2).

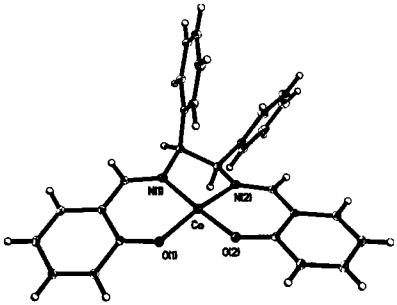

Figure 7. Thermal ellipsoid plot (50% probability level) of Co(MDEDS).

Selected bond	Length (Å)
Co-N(1)	1.8575 (14)
Co-N(2)	1.8666 (14)
Co-O(2)	1.8405 (12)
Co-O(1)	1.8463 (12)
N(1)-C(8)	1.482 (2)
C(1)-C(2)	1.415 (2)

Table 1. Selected bond distances in Co(MDEDS).

Selected bond	Angle (°)
O(2)-Co-O(1)	85.92 (5)
O(2)-Co-N(1)	173.34 (6)
O(1)-Co-N(1)	94.47 (6)

Table 2. Selected bond angles in Co(MDEDS).

The O-Co-O and O-Co-N bonds in which the two atoms bound to the metal center were positioned cis to one another were believed to be in square planar orientation. Bond angles close to 90 degrees indicate that this is the approximate geometric configuration of the ligand frame.

Co(MDEDS) was also characterized using UV/ VIS absorption spectroscopy. This technique involved dissolving the complex in methylene chloride and taking absorption spectra. Quantitative UV/VIS studies were performed and Beer's Law plots were created in order to determine the molar extinction coefficients at select wavelengths. Quantitative UV/VIS absorption spectra of Co(MDEDS) in methylene chloride were generated (Figure 8). UV/VIS data were also collected in methylene bromide. The absorption spectrum is shown in Figure 9.

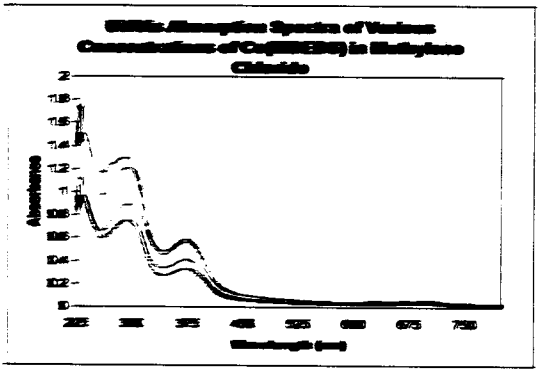

Figure 8. UV/VIS absorption spectra of Co(MDEDS) in methylene chloride at concentrations of 5.47×10^{-5}, 4.61×10^{-5}, 4.03×10^{-5}, 3.46×10^{-5}, 2.88×10^{-5} M.

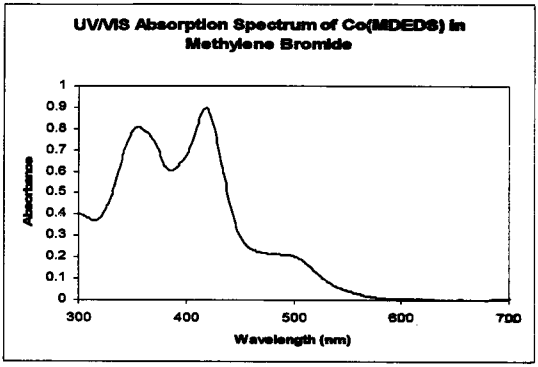

Figure 9. UV/VIS absorption spectrum of Co(MDEDS) in methylene bromide.

The great differences in the peak shapes in these spectra are associated with different solvent interactions that occur as a result of changing an atom in the solvent from chloride to bromide. Extinction coefficients were determined at the three maximal wavelengths in each of the solvents (Table 3).

Solvent	λ_{max} (nm)	ε ($M^{-1}cm^{-1}$)
Methylene Chloride	272	22452
Methylene Chloride	291	24677
Methylene Chloride	373	12072
Methylene Bromide	356	13867
Methylene Bromide	365	13261
Methylene Bromide	418	15432

Table 3. Extinction coefficients for Co(MDEDS) at maximal wavelengths.

[Co_2(MDEDS)$_2Cl_2$)] Synthesis

Cobalt (II) has a strong propensity to air oxidize to the cobalt (III) oxidation state in the presence of strong field ligands. When the Co(MDEDS) synthesis was carried out aerobically, oxidation occured. A dimeric cobalt species ligated to two MDEDS ligands was formed. This species was crystallized in the same fashion as the Co(MDEDS) complex and analyzed using x-ray diffraction (Figure 10).

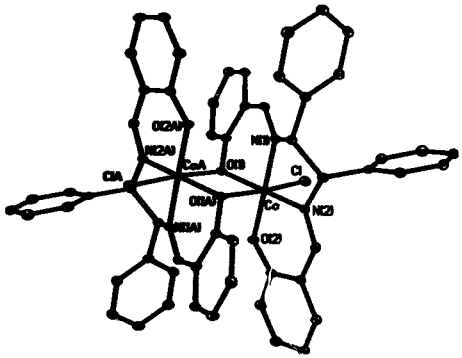

Figure 10. Thermal ellipsoid plot (50% probability level) of $Co_2(MDEDS)_2Cl_2$.

The $Co_2(MDEDS)_2Cl_2$ complex contains two cobalt (III) metal centers with octahedral geometry. The metal centers are each ligated to one MDEDS ligand with one of the phenolate oxygen atoms bridging to the adjacent Co(III) center. A single chloride ion in each completes the coordination sphere. Select bond distances and angles for this complex are shown (Table 4 and Table 5).

Selected bond	Length (Å)
Co-N(1)	1.8917 (16)
Co-N(2)	1.8846 (17)
Co-O(2)	1.8754 (14)
Co-O(1)	1.9312 (14)
C(1)-C(2)	1.393 (3)

Table 4. Selected bond distances in $[Co_2(MDEDS_2Cl_2)]$.

Selected bond	Angle (°)
O(2)-Co-N(2)	96.40 (7)
O(2)-Co-N(1)	178.46 (7)
O(1)-C(1)-C(2)	119.43 (18)
O(1)-C(1)-C(6)	121.36 (18)
O(1)-Co-Cl	92.66 (4)

Table 5. Selected bond angles in $[Co_2(MDEDS_2Cl_2)]$.

The bond angles close to 90 and 180 degrees are indicative of square planar geometries. Those near 120 degrees are indicative of trigonal planar geometry.

♠ **$[Co(MDEDS)(CN)_2]$ Synthesis**

A reaction between Co(MDEDS) and tetraethylammonium cyanide was carried out in acetonitrile. After combining the two substances, the reaction was set to reflux for 1.5 h. Reflux caused the reaction to proceed as evidenced by the color change from dark brown to red.

Spectroscopic studies provided further evidence that the reaction went to completion. The infrared spectrum in Figure 11 was collected.

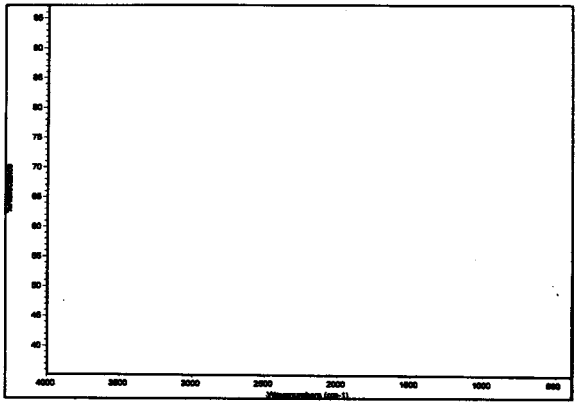

Figure 11. IR spectrum of $Co(MDEDS)CN_2$.

The sharp peak at 2122 cm^{-1} in the IR spectrum is assigned to a cyanide stretch ($\nu_{C\equiv N}$). This peak is shifted from 2080 cm^{-1}, the frequency at which unbound cyanide is expected to stretch. The shift to a higher frequency indicates that the cyanide acts as a ligand to the metal center.

♠ $(Et_4N)_2[Co(PyPS(SO_2))]_2$ Synthesis

The starting material $(Et_4N)_2[Co_2(PyPS)_2]$ was synthesized according to the procedure published by Mascharak et al.[25] This dimeric species is symmetric and thus not useful in coupling constant analyses. Hence a reaction between $(Et_4N)_2[Co_2(PyPS)_2]$ and hydrogen peroxide was undertaken to introduce asymmetry to the complex (Scheme 3).

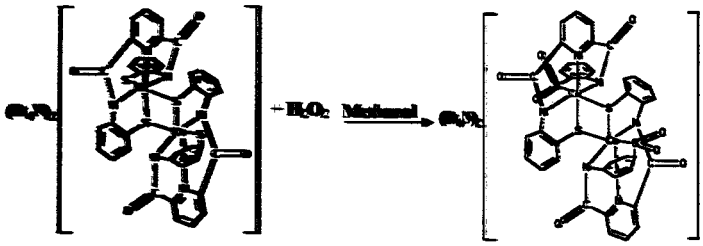

Scheme 3. Synthesis of $(Et_4N)_2[Co(P_2PS(SO_2))]$.

Addition of H_2O_2 to the dimer causes oxidation of the terminal thiolates. The bridging thiolates remained unmodified. The reactivity differences between the two thiolates can be attributed to differences in the electron density. The bridging thiolates are involved in three chemical bonds and their electron density is more distributed than that of the terminal thiolates which are involved in just two chemical bonds. The terminal thiolates contain lone pairs which are susceptible to attack by the peroxide oxygen atoms. Thus, the terminal thiolates are selectively oxidized.

It is important, however, that the product be collected after 2 h of stirring. This is necessary in order to maintain the specificity of the oxidation. Reactions that were left stirring longer resulted in an increase in impurities attributed to over oxidation of the product.

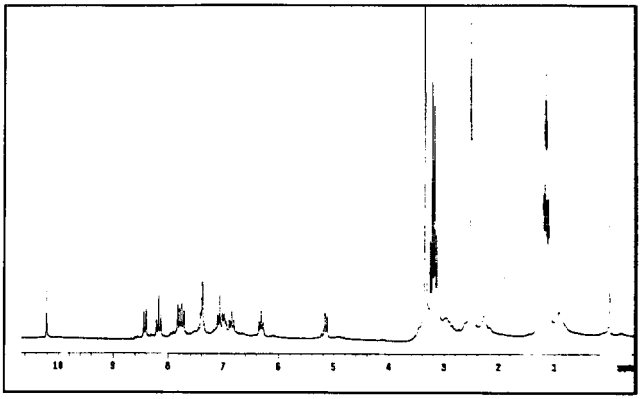

Figure 12. ^{1}H NMR of $(Et_4N)_2[Co(PyPS(SO_2))]_2$ in DMSO on a 200MHz instrument.

This ^{1}H NMR spectrum of $(Et_4N)_2[Co(PyPS(SO_2))]_2$ (Figure 12) is well defined indicating that the product is pure. The resonance at 5.2 ppm results from the interaction of the thiol aromatic ring and the pi electrons on the second thiol ring ligated to the other cobalt (III). This peak was seen in the unoxidized dimer, and provides evidence that the product has maintained its dimeric structure.

♣ $(Et_4N)_3[Co(PyPS(SO_2))(CN)_2]$ Synthesis

The dicyano complex of the oxidized dimer was obtained by a reaction of $(Et_4N)_2[Co(PyPS(SO_2))]_2$ with six equivalents of NEt_4CN. This reaction was carried out in anhydrous acetonitrile. The NEt_4CN was used to break the dimer into two equivalent monomeric species. This complex contains cyanide ligands in both axial positions and the $PyPS^{-4}$ ligand occupies the four equatorial positions. The CN^- is a strong ligand and is capable of breaking the thiolate bridge between the cobalt metal centers. The synthetic

pathway followed to obtain the $(Et_4N)_3[Co(PyPS(SO_2))(CN)_2]$ complex is shown (Scheme 4).

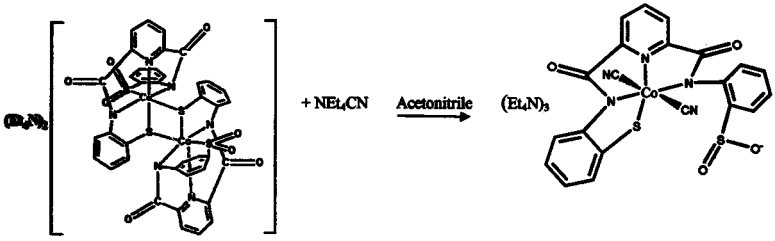

Scheme 4. Synthesis of $(Et_4N)_3[Co(PyPS(SO_2))(CN)_2]$.

An infrared spectrum of the product of this reaction contains a stretching frequency at 2120 cm^{-1} (Figure 13). As was the case with the MDEDS dicyano complex, the $\nu_{C\equiv N}$ peak is shifted from that of unbound cyanide, indicating the cyanide has ligated to the metal center.

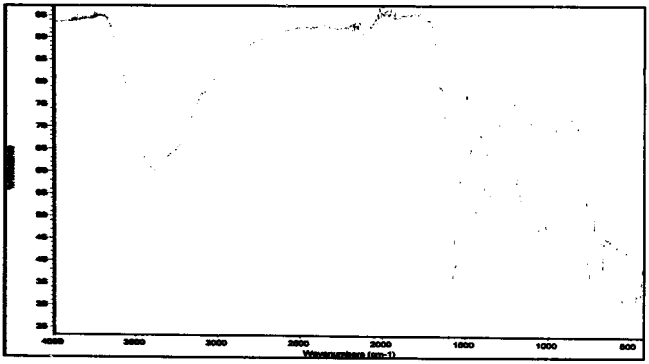

Figure 13. IR spectrum of $(Et_4N)_3[Co(PyPS(SO_2))(CN)_2]$.

The ^{1}H NMR spectrum of [illegible] revealed that the peak at ~5.2 ppm is missing, indicating that the species is monomeric (Figure 14).

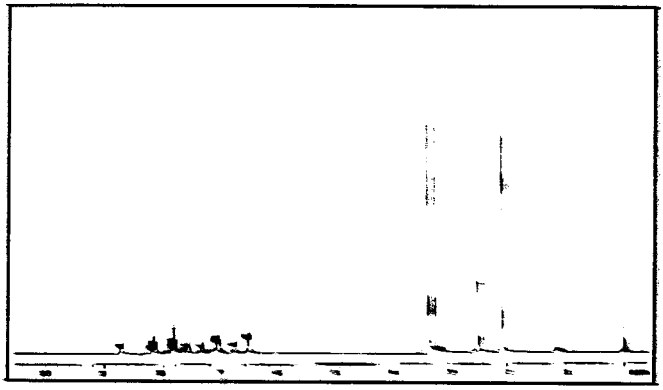

Figure 14. ^{1}H NMR spectrum of [illegible] in DMSO on a 200 MHz instrument.

Following the successful synthesis and characterization of the $(Et_4N)_2[Co(PyPS(SO_2))(CN)_2]$ complex, an analogous reaction was carried out with ^{13}C enriched $NEt_4{}^{13}CN$. The ^{13}C NMR spectrum for this complex is shown (Figure 15).

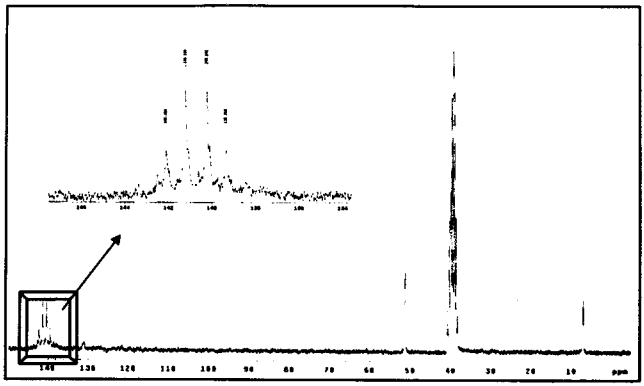

Figure 15. ^{13}C NMR spectrum of $(Et_4N)_3[Co(PyPS(SO_2))(^{13}CN)_2]$ in DMSO on a 200 MHz instrument.

Due to the asymmetry imparted by the oxidized thiolates, the cyanide ligands in the complex are in dissimilar chemical environments. This can be seen in Figure 16, a pictorial representation of the complex. Each of the axial cyanide ligands will give rise to separate resonances in the NMR spectrum. These two signals are shown as the two sets of doublets at 139.8 ppm and 141.7 ppm. The inset within Figure 15 shows the doublets enlarged. This is one of the first reported cases of through metal coupling of ^{13}C nuclei.

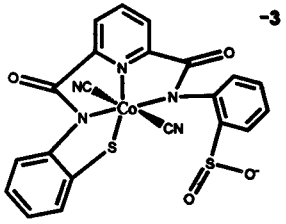

Figure 16. $[Co(PyPS(SO_2))(^{13}CN)_2]$

♠ Future Work

To date the completion of the $Co(MDEDS)CN_2$ reaction is only evidenced through the qualitative color change and a changed infrared spectrum. NMR studies have yet to provide insightful results. A proton NMR spectrum has been collected, but no ^{13}C NMR data has been acquired. The future of this project involves collecting a ^{13}C NMR spectrum.

The next step in the project will involve the synthesis of an analogous complex in which isotopically enriched $NEt_4{}^{13}CN$ is used in place of the non-isotopically labeled equivalent. Once the product is isolated, the ^{13}C NMR spectrum associated with this complex will be collected. If through metal coupling is observed a $^2J_{C\text{-}C}$ will be calculated and reported.

Additionally, different isotopically labeled ligands will be introduced. For example, complexes containing $S^{13}CN^-$ will be investigated. A series of studies can be done in this respect, given that complexes containing multiple $S^{13}CN^-$ ligands will be synthesized, as well as those containing one $S^{13}CN^-$ and one $^{13}CN^-$ ligand.

The future of the MDEDS segment of the project has potential to be very far reaching. It is expected that other metal centers will be studied. Specifically, it is likely that the diamagnetic, d^{10} configured, zinc (II) will be investigated.

Appendix A

Table of Contents

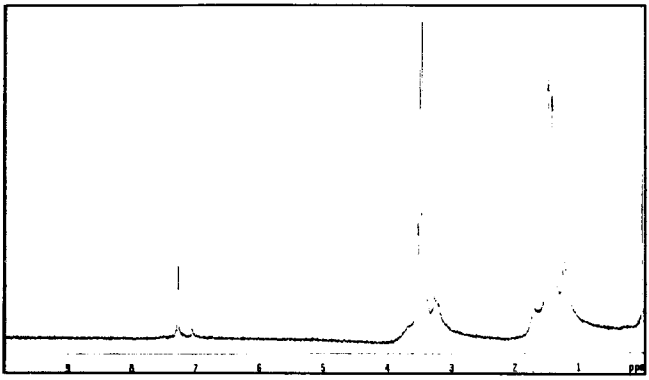

A-1. ^{1}H NMR spectrum of $Et_4NS^{13}CN$ in $CDCl_3$ on a 200 MHz instrument.

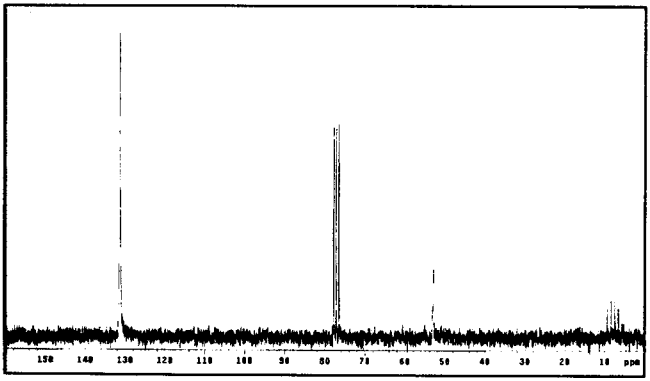

A-2. ^{13}C NMR spectrum of $Et_4NS^{13}CN$ in $CDCl_3$ on a 200 MHz instrument.

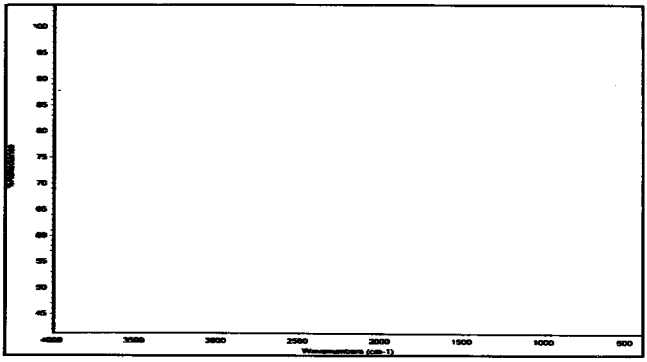

A-3. IR spectrum of Et_4NSCN.

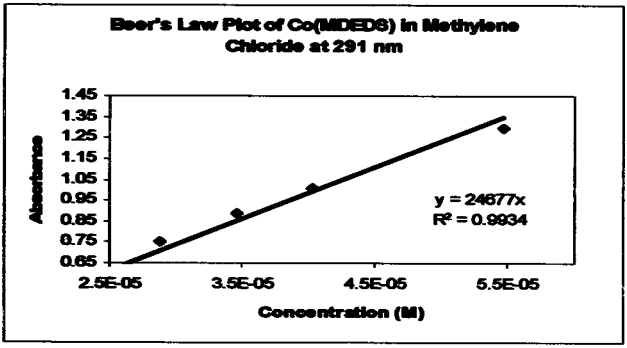

A-4. Beer's Law Plot of Co(MDEDS) in methylene chloride at 291nm.

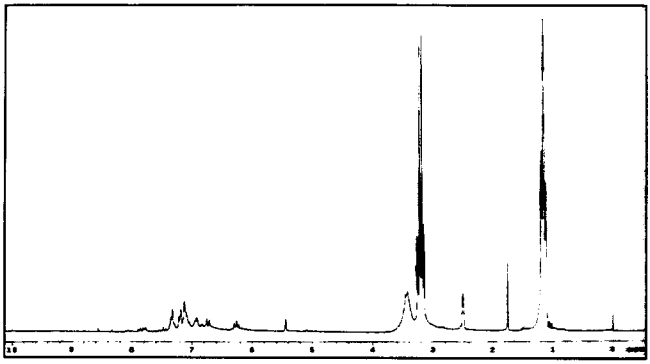

A-5. ^{1}H NMR spectrum of $Co(MDEDS)CN_2$ in DMSO on a 200 MHz instrument.

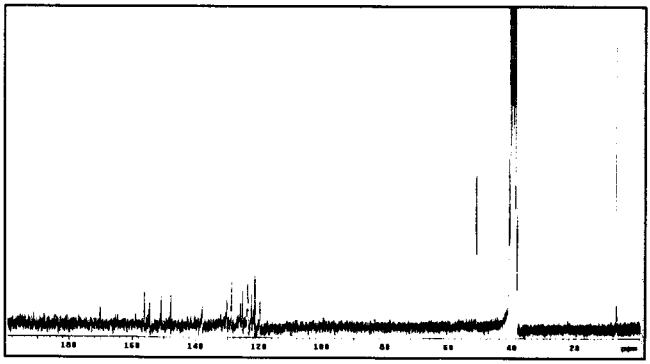

A-6. ^{13}C NMR spectrum of $(Et_4N)_2[Co(PyPS(SO_2))]_2$ in DMSO on a 200 MHz instrument.

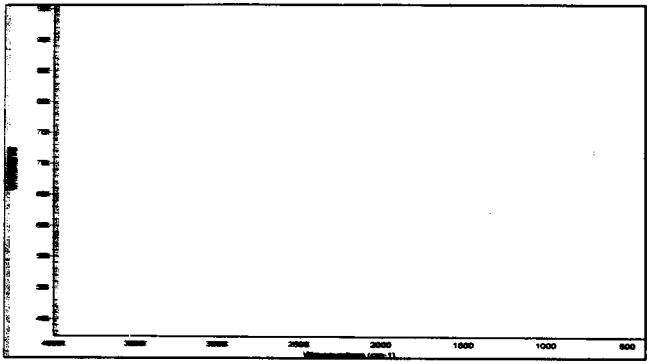

AZ. IR spectrum of $(Et_4N)_2[Co(PyPS(SO_2))]_2$.

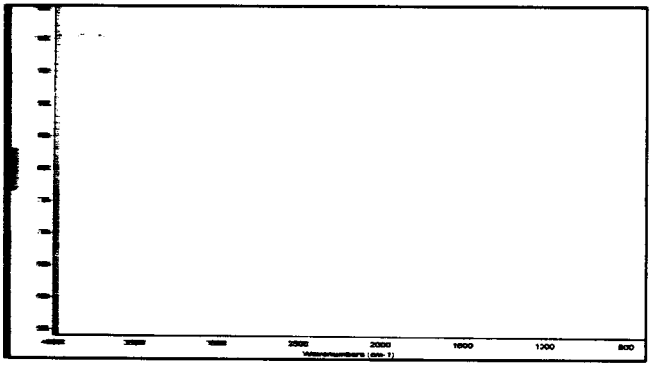

BR. IR spectrum of $NEt_4^{15}CN$.

REFERENCES

1. Cavanagh, J.; Fairbrother W. J.; Palmer III A. G.; Skelton N.J. *Protein NMR Spectroscopy: Principles and Practice*, 2nd Edition, Academic Press **2006**.
2. Pelczer, I. *NMR in Ligand Screening: Theory, Methods, and Applications*, Oxford University Press **2006**.
3. Ding, K; Gronenborn, A. M. *J. Am. Chem. Soc.* **2004**, *126*, 6232.
4. Van Melckebeke, H.; Simorre, J. P.; Brutscher, B. *J. Am. Chem. Soc.* **2004**, *126*, 9584.
5. Machonkin, T. E.; Westler, W. M.; Markley, J. L. *J. Am. Chem. Soc.* **2002**, *124*, 3204.
6. Phan, A. T; Patel, D. J. *J. Am. Chem. Soc.* **2002**, *7*, 1160.
7. Olsen, R. A.; Struppe, J.; Elliott, D. W.; Thomas, R. J.; Mueller, L. J. *J. Am. Chem. Soc.* **2003**, *125*, 11784.
8. Robinson, J.W.; Skelley Frame, E.M.; Frame II, G.M. *Undergraduate Instrumental Analysis*, Sixth Edition, Marcel Dekker **2005**.
9. Bryce, D.L.; Wasylishen, R. E. *Inorg. Chem.* **2002**, *41*, 4131.
10. Kofod, P.; Harris, P.; Larsen, S. *Inorg. Chem.* **1997**, *36*, 2258.
11. Wylie, B.J.; Sperling, L.J.; Frericks, H.L.; Shah, G.J.; Franks, W.T.; Rienstra, C.M. *J. Am. Chem. Soc.* **2007**, *129*, 5318.
12. Wang, Y.; Lawler, D.; Larson, B.; Ramadan, Z.; Kochhar, S.; Holmes, E.; Nicholson, J.K. *J. Proteome Res.* **2007**, *6*, 1846.
13. Pochapsky, S.S.; Pochapsky, T.C. *Curr. Top. Med. Chem.* **2001**, *1*, 427.
14. Moon, R. B.; Richards, J. H. *Biochemistry* **1974**, *13*, 3437.
15. Fujii, H. *J. Am. Chem. Soc.* **2002**, *124*, 5936.
16. Watzky, M.A.; Endicott, J.F.; Song, X.; Lei, Y.; Macatangay, A. *Inorg. Chem.* **1996**, *35*, 3463.
17. Huang, Hui.; Alvarez, K.; Lui, Q.; Barnhart, T.M.; Snyder, J.P.; Penner-Hahn, J.E. *J. Am. Chem. Soc.* **1996**, *118*, 8808.
18. Puerta, D.; Cohen, S. *Inorg. Chem.* **2002**, *41*, 5075.
19. Safo, M.K.; Gupta, G.P.; Watson, C.T.; Simonis, U.; Walker, F. A.; Scheidt, W. R. *J. Am. Chem. Soc.* **1992**, *114*, 7066.
20. Safo, M.K.; Walker, F. A.; Raitsimring, A. M.; Walter, W. P.; Dolata, D. P.; Debrunner, P. G.; Scheidt, W. R. *J. Am. Chem. Soc.* **1994**, *116*, 7760.
21. Nakamura, M.; Ikeue, T; Fujiii, H.; Yoshimura, T. *J. Am. Chem. Soc.* **1997**, *119*, 6284.
22. Ye, B. H.; Li, X. Y.; Williams, I. D.; Chen, X. M. *Inorg. Chem.* **2002**, *41*, 6426.
23. Chow, C.; Lam, M.H.W.; Wong, W. Inorg. Chem. **2004**, *43*, 8387.
24. Noveron, J.C., Olmstead, M.M., Mascharak, P.K., *J. Am. Chem. Soc.* **1999**, *121*, 3553.
25. Tyler, L, Noveron, J.C., Olmstead, M.M., Mascharak, P.K., *Inorg. Chem.* **2003**, *42*, 5751.